

PAPER • OPEN ACCESS

## Experimental analysis of WEDM machined surface of Inconel 825 using single objective PSO

To cite this article: P Kumar *et al* 2019 *J. Phys.: Conf. Ser.* **1240** 012053

View the [article online](#) for updates and enhancements.

You may also like

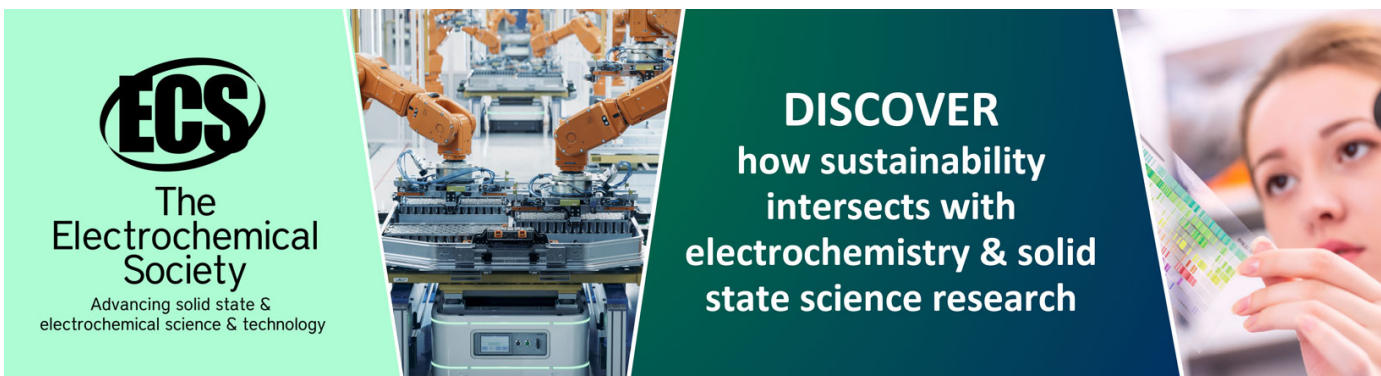
- [Investigations on the influence of particle reinforcement and wire materials on the surface quality and machining characteristics of AA6061-TiB<sub>2</sub> alloy in WEDM](#)

K Ramraji, K Rajkumar, G Selvakumar et al.

- [Surface and subsurface investigation of Al-Mg-MoS<sub>2</sub> composite on performing wire electrical discharge machining](#)

Senthil Kumar S, Sudhakara Pandian R, Pitchipoo P et al.

- [Investigations on wire electric discharge machining of hybrid nano metal matrix composites \(AA6061/SiC/B<sub>4</sub>C\) for industry need based multi-response optimization](#)  
Shubhajit Das, M Chandrasekaran and S Samanta



**ECS**  
The  
Electrochemical  
Society  
Advancing solid state &  
electrochemical science & technology

**DISCOVER**  
how sustainability  
intersects with  
electrochemistry & solid  
state science research

# Experimental analysis of WEDM machined surface of Inconel 825 using single objective PSO

P Kumar<sup>1\*</sup>, M Gupta<sup>1</sup> and V Kumar<sup>2</sup>

<sup>1</sup>Department of Mechanical Engineering, NIT, Kurukshetra

<sup>2</sup>Department of Mechanical Engineering, UIET, Maharishi Dayanand University, Rohtak  
[nain.pawan2@gmail.com](mailto:nain.pawan2@gmail.com)

**Abstract.** The present research focuses on the analysis of surface topography of Inconel 825 superalloy, machined with Wire Electrical Discharge Machining. Surface texture analysis includes cracks, craters, pockmarks, heat affected zone and recast layer thickness. Particle swarm optimization used response surface methodology (RSM) to find the optimum combination of WEDM characteristics *viz.* pulse on time, pulse off time, gap voltage, peak current, wire tension and wire feed. Surface crack density (SCD) and recast layer thickness (RCL<sub>t</sub>) are the output responses. The results manifest that pulse on time, peak current and gap voltage are the most influential parameters for surface topography. At optimum combination of process parameters, the value obtained for SCD is 0.000423  $\mu\text{m}/\mu\text{m}^2$  and RCL<sub>t</sub> is 8.044  $\mu\text{m}$ . Under optimized conditions, surface topography of the machined specimen is improved that makes it suitable for implementation in industry.

**Keywords:** WEDM; Inconel 825; Surface crack density; Recast layer thickness; RSM; PSO

## 1. Introduction

Superalloys are complex materials having resistance to high temperature and corrosion. Nickel-based superalloys are the most multifaceted widely used alloys for the hottest parts of advanced aircraft engines. [1]. Inconel 825 is Ni-Fe-Cr alloy with inclusion of Mo, Cu and Ti [2]. It has an austenitic structure that imparts high ductility and work hardening properties. Inconel 825 has the tendency to get it welded on the cutting tool during cutting and formation of built-up edges makes it difficult to machine with conventional methods [3]. WEDM is best alternative for making intricate shapes and profiles with superior surface finish and accurate dimensions for hard and tough material like Inconel 825 [4].

The exactitude of material surface has always been a matter of concern during machining. Surface parameters including surface roughness, residual stresses, micro-hardness and microstructure are crucial in determining the final performance of the machined specimen [5]. Very high temperature (8000-12000°C), that occurred in WEDM results in consequential impact on the surface roughness of the machined specimen. The material which cannot be removed by the dielectric flush re-solidifies on the surface and creates a recast layer. This process also leads to stress resulting in the formation of cracks and pores on the surface, thus damages the surface integrity [6]. Surface integrity of a machined sample is closely related to the surface quality of the work material and thus contributes to its mechanical properties.

Various studies have been reported on surface integrity studies of WEDM machined steels [7] and nickel-based superalloys [8]. The recast layer formation on the top surface of machined specimen depends upon the process condition and work-piece properties. It is evident from the literature study that discharge energy is the most influencing parameter for surface integrity characteristics. Puri and Bhattacharyya [9] employed RSM approach to study effects of input variables on depth of white layer during WEDM process. It was observed that the white layer depth (WLD) increases with increase in pulse-on time during first cut, while a sharp decrease was found with increase in pulse-on time during trim cut.



Rajyalakshmi and Venkata Ramaiah [10] explored the effect of input parameters of WEDM on surface roughness (SR) of Inconel-825. Significant improvement in surface finish ( $1.36\mu\text{m}$ ) was observed at low values of WF (2m/min),  $T_{\text{on}}$  (110  $\mu\text{s}$ ) and gap voltage (20V). At high value of discharge energy, surface irregularities increased because more materials melted and re-solidification on the surface. Caydas and Ay [11] presented an investigation of WEDM characteristics on cutting quality of an annealed Inconel 718. On the basis of ANOVA test it was found that intensity of the current and pulse duration affects the cutting quality significantly in terms of surface roughness, kerf width and  $RCL_t$  whereas injection pressure of liquid had little effect on the surface roughness, recast-layer thickness and kerf width. Talla and Gangopadhyay [12] showed that addition of silicon powder in dielectric significantly improves the surface integrity during machining of Inconel 625. With the use of silicon powder lowest surface roughness and smallest amount of residual stress were obtained.

Goyal [13] observed major changes on the surface of Inconel 625 specimen after WEDM machining with cryogenically treated tool electrode and zinc coated tool electrode. The microstructure analysis of surface included globules of debris, melted drops, cracks and craters. Because of low melting temperature and high heat conductivity, the cryo-treated tool electrode produced better surface quality for Inconel 625 alloy. In another work, Sharma et al. [14] evaluated the microstructure analysis of Inconel 706 and found that the machined surface was composed of melted debris and micro holes but no microcracks were detected due to the high toughness of the alloy. The best surface quality was obtained at low value of  $T_{\text{on}}$  and high value of  $T_{\text{off}}$ . A thick recast layer (39.6  $\mu\text{m}$ ) was observed at high value of pulse on time and low value of servo voltage.

Many authors have studied the surface integrity of the machined samples under optimized conditions. There are very few studies where surface integrity was studied in terms of surface crack density (SCD) and recast layer thickness ( $RCL_t$ ) and machining parameters were optimized to reduce the surface roughness [6]. This research mainly focuses on optimization of machining parameters on surface roughness (SR) of machined specimens in terms of SCD and  $RCL_t$  using WEDM. A nature inspired metaheuristic algorithm called particle swarm optimization (PSO) is used for the optimization of WEDM machining parameters.

## 2. Material and Method

### 2.1 Specimen and Mechanism of WEDM

In the present research, Inconel 825 was used as experimental work material having 150 mm length, 150 mm breadth and 10 mm thickness as shown in Figure 1a. The Chemical composition of work material was Nickel 38-46%, Chromium 19.5-23.5%, Ferrous 22 %, Molybdenum 2.5-3.5%, Copper 1.5-3.0%, Titanium 0.6-1.2%, Magnesium 1.0%, Carbon 0.05%, Sulphur 0.03% and Phosphorus 0.02%. With the WEDM process a specimen of (5 × 5 × 10) mm is cut from the work material as shown in Figure 1b.

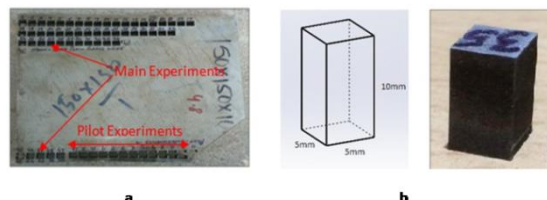


**Figure 1.** WEDM machining of Inconel 825 (a) work material (b) specimen after machining

All experiments are performed using CNC WEDM machine tool (ELECTRA SPRINT CUT 734) in Mechanical Engineering Department, N.I.T. Kurukshetra, India. A plain brass wire (diameter = 0.25mm) was used as tool electrode. WEDM is a thermo-electric spark erosion process in which material is melted in the suitable gap of 0.025 - 0.5 mm between tool and workpiece electrode. Under the action of electric field, the gap voltage reaches the breakdown voltage and spark is generated between the electrodes gap. The temperature in the smallest gap where plasma zone occurs, is around

8000-10000°C. The debris produced during machining is flushed by the dielectric fluid pressure as shown in Figure 2.

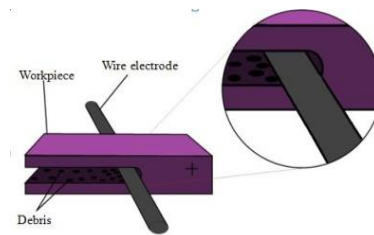


**Figure 2.** Mechanism of Wire cut EDM process

## 2.2 Experimentation

Response surface methodology (RSM) is a mathematical approach used to models, improve and optimize different process parameters. RSM develop a regression model which identifies the interaction between the input variables and output responses. Input parameters used are pulse on time ( $T_{on}$ ), pulse off time ( $T_{off}$ ), peak current (IP), gap voltage (SV), wire tension (WT) and wire feed (WF). The ranges were selected on the basis of the results obtained from the preliminary investigations and literature search [2]. The microstructural response characteristics were measured in term of SCD and  $RCL_t$ .

## 2.3 Measurements of surface characteristics

All measurement related to surface micrograph were performed on JEOL Scanning Electron Microscope (Model 6100, JEOL, USA); a profile measuring microscope that determines the surface microstructure, formation of SCD and  $RCL_t$  of the work material machined with WEDM. Etching process of machined sample was carried out with krolls reagent (2% (v/v)) hydrofluoric acid, 10% ((v/v) nitric acid). Then, acetone ( $CH_3)_2CO$  was used to clean the samples to observe the samples under scanning electron microscope.

Axio-vision software was used to measure the SCD and  $RCL_t$ . SEM micrograph of each specimen was imported in the axio-vision software and surface cracks were measured by obtaining the length of the cracks on each specimen. Surface crack density is the ratio of average length of cracks to area of the given micrograph. Due to rapid quenching process, a multilayered surface was developed during cutting operation. At very top an appearance was observed on work surface known as recast layer.  $RCL_t$  is the ratio of length of recast layer to the area of recast layer.

SCD and  $RCL_t$  can be calculated by using Equation 1 and 2 respectively.

$$SCD = LC / A \quad \dots (1)$$

where, SCD = Surface crack density; LC = Average Length of the crack ( $\mu\text{m}$ ); A = Area of the micrograph ( $\mu\text{m}^2$ )

$$RCL_t = RCLA / RCL \quad \dots (2)$$

where,  $RCL_t$  = Recast layer thickness ( $\mu\text{m}$ ); RCLA = Recast layer area ( $\mu\text{m}^2$ ); RCL = Recast layer length ( $\mu\text{m}$ )

## 2.4 Design of Experiment

The ranges of input parameters are divided into five levels. Design expert (version 9.0.7, Statease) was used for RSM and central composite design (CCD) system at  $\alpha$  value of  $\pm 2$  was used. Response Surface Methodology (RSM) is a collection of statistical and mathematical techniques useful for developing, improving, and optimizing the processes. The most extensive applications of RSM are to minimize variability in the output response of a product or to process around a target value. RSM based particle swarm optimization algorithm was used to optimize the responses. A regression equation was generated that results in an empirical model which relates the output responses to the process variables of the experiment.

$$y = \beta_0 + \sum_{i=1}^k \beta_i x_i + \sum_{i=1}^k \sum_{j=1, i < j}^k \beta_{ij} x_i x_j + \sum_{i=1}^k \beta_{ii} x_i^2 + \varepsilon \quad \dots (3)$$

where,  $y$  is the predicted response [SCD, RCL<sub>t</sub>],  $x_i, x_j$  are the independent variables,  $\beta_0$  is intercept coefficient,  $\beta_i$  are the regression coefficients of zero order,  $\beta_{ij}$  is the squared coefficients.. Equation 3 was used to create 3D plots.

### 2.5 Single objective particle swarm optimization

Particle swarm optimization was a metaheuristic approach that uses nature based algorithm for optimization. The algorithm was developed by James Kennedy Russell Eberhart in 1995 [15]. It is a swarm intelligence based optimization technique in the field of machine learning to find the optimum solution. PSO is a population based method in which each  $i^{\text{th}}$  particle is a candidate solution and represented by its velocity ( $v_i$ ) and position ( $x_i$ ). Particles change their position in multi dimensional space ( $d$ ) by flying. By changing its velocity, new position of the particle arises i.e.  $x_i = (x_{i1}, x_{i2}, \dots, x_{id})$ . In each iteration particle adjusts its position according to own best position ( $p_{best}$ ) and global best position ( $g_{best}$ ) i.e. experience of neighboring particles. Therefore, a new velocity value for each particle is intended based on its existing velocity and modified velocity value was used to calculate the next position of each particle in multi dimensional space. This procedure was repeated number of times for updation of velocity and position and stop iteration when minimum error is achieved. PSO is stochastic optimization technique based on the movement and intelligence of swarms. The following steps were used in PSO algorithm:

Step 1. Randomly create the initial population of the particles ( $x$ ) over multi-dimensional space ( $d$ ).

Step 2. For each particle, value of objective function was calculated.

Step 3. For each particle find out best position it has visited so far. Let it be  $p_{best}$ . Also find out the best position obtained so far by any particle in the population i.e.  $g_{best}$ .

Step 4. Find modified velocity of each particle by using the equation 4 and 5

$$v_{id}^{j+1} = w \times v_{id}^{j+1} + c_1 \times r_1 \times (p_{best_i} - x_{id}^j) + c_2 \times r_2 \times (g_{best_i} - x_{id}^j) \quad \dots (4)$$

$$w = w_{max} - \frac{w_{max} - w_{min}}{iter_{max}} \times (j + 1) \quad \dots (5)$$

Where  $c_1$  and  $c_2$  are the constant,  $r_1$  and  $r_2$  are random numbers in the range [0-1],  $w$  is the inertia weight and  $j$  is the iteration number and  $iter_{max}$  is the maximum number of iterations

Step 5. Update particle's current position by using the Equation 6

$$x_{id}^{j+1} = x_{id}^j + v_{id}^{j+1} \quad \dots (6)$$

Step 6. Compare the new objective function value of each particle with previous one.

If solution improves: Keep this position, otherwise

$$x_{id}^{j+1} = x_{id}^j$$

Step 7. If the numbers of iteration reaches to the maximum value then go to step 8 otherwise go to step 4.

Step 8. Latest  $g_{best}$  is the solution of the problem

### 2.6 Validation of the predicted model

To ensure the validity of the chosen model, experiments were designed using the predicted optimum values of the parameters. The responses were measured and compared with the predicted value.

## 3. Result and Discussion

In the present research, input parameters like  $T_{on}$ ,  $T_{off}$ , IP, SV, WT and WF were chosen on the basis of preliminary investigations and literature search. A total of 52 experiments as suggested by RSM were conducted as shown in Table 1. SEM analysis was carried out for each 52 runs.

**Table 1.** Central composite design with actual responses

Run	T <sub>ON</sub> (Machine unit)	T <sub>OFF</sub> (Machine unit)	SV (V)	IP (Amp)	WT (Machine unit)	WF m/min	SCD ( $\mu\text{m}/\mu\text{m}^2$ )	RCL <sub>t</sub> ( $\mu\text{m}$ )
1	111	38	50	130	10	4	0.0058	24.89
2	111	38	50	130	10	6	0.0073	25.03
3	109	35	54	140	11	7	0.0087	26.83
4	113	35	54	120	11	7	0.0081	25.67
5	113	41	54	120	9	7	0.0110	24.43
6	113	35	54	120	9	5	0.0059	26.56
7	113	41	46	140	9	7	0.0130	30.30
8	111	38	50	130	10	6	0.0073	23.89
9	109	41	46	120	9	7	0.0028	21.96
10	109	35	54	140	9	5	0.0061	22.99
11	109	41	46	140	11	5	0.0068	25.80
12	109	41	54	140	9	7	0.0063	22.83
13	109	41	46	140	9	5	0.0047	22.40
14	113	35	46	120	9	7	0.0100	28.20
15	111	38	50	130	10	6	0.0082	24.02
16	111	38	50	130	10	6	0.0073	25.87
17	109	35	46	140	9	7	0.0065	25.61
18	115	38	50	130	10	6	0.0138	34.62
19	113	35	46	140	11	7	0.0110	28.89
20	111	32	50	130	10	6	0.0085	26.70
21	111	44	50	130	10	6	0.0068	24.13
22	113	35	54	140	11	5	0.0091	30.85
23	109	41	54	140	11	5	0.0068	25.89
24	111	38	50	130	10	6	0.0075	24.13
25	113	41	46	120	11	7	0.0078	22.71
26	109	35	46	120	9	5	0.0051	23.56
27	109	35	54	120	11	5	0.0038	23.67
28	111	38	50	130	8	6	0.0077	25.66
29	111	38	50	150	10	6	0.0127	29.27
30	109	35	54	120	9	7	0.0022	20.47
31	113	41	54	140	11	7	0.0140	31.16
32	111	38	50	130	12	6	0.0070	25.17
33	111	38	50	130	10	6	0.0070	24.04
34	109	35	46	140	11	5	0.0083	22.90
35	111	38	50	130	10	6	0.0072	25.01
36	111	38	42	130	10	6	0.0069	24.59
37	113	41	54	140	9	5	0.0130	30.74
38	109	41	46	140	11	7	0.0046	23.74
39	109	41	54	120	9	5	0.0034	20.51
40	113	41	54	120	11	5	0.0069	24.93
41	109	41	54	120	11	7	0.0051	22.66
42	109	35	46	120	11	7	0.0053	23.61
43	111	38	58	130	10	6	0.0082	26.24
44	113	41	46	120	9	5	0.0073	26.08
45	113	35	46	120	11	5	0.0061	23.84
46	107	38	50	130	10	6	0.0014	20.05
47	111	38	50	130	10	8	0.0085	25.94
48	113	35	46	140	9	5	0.0110	31.06

49	113	35	54	140	9	7	0.0120	31.08
50	111	38	50	130	10	6	0.0072	25.32
51	109	41	46	120	11	5	0.0018	20.89
52	111	38	50	110	10	6	0.0023	21.55

Figure 3 shows the SCD and  $RCL_t$  values of different runs which were calculated by Axio vision software. The SEM micrographs of different runs showed the presence of craters, pockmarks, heat affected zone, recast layer and pulled out material as shown in Figure 3.

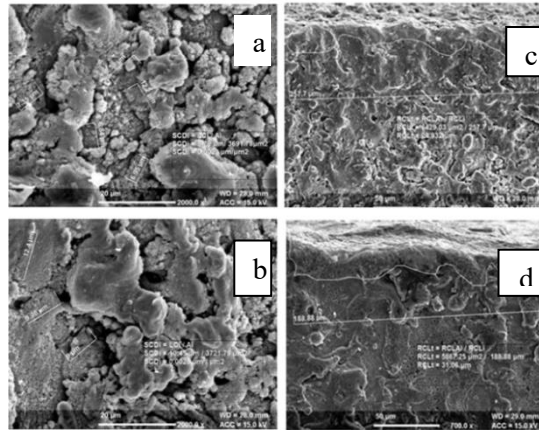


**Figure 3.** Surface crack density at (a) Exp no.52 (b) Exp no. 9 and recast layer thickness at (c) Exp no.40 (d) Exp no.48

The Analysis of variance test of Surface crack density is shown in Table 2.

**Table 2.** ANOVA test for surface crack density (SCD)

Source	Sum of Squares	df	Mean Square	F Value	p-value Prob > F	
Model	0.000455	21	2.17E-05	73.64428	< 0.0001	significant
Pulse on Time-A	0.000235	1	0.000235	798.6885	< 0.0001	
Pulse off Time-B	1.42E-06	1	1.42E-06	4.826799	0.0359	
Gap Voltage-C	4.08E-06	1	4.08E-06	13.86238	0.0008	
Peak Current-D	0.000126	1	0.000126	428.911	< 0.0001	
Wire Tension-E	1.43E-06	1	1.43E-06	4.853403	0.0354	
Wire Feed-F	1.92E-05	1	1.92E-05	65.17797	< 0.0001	
AB	9.03E-06	1	9.03E-06	30.69264	< 0.0001	
AC	4.51E-07	1	4.51E-07	1.53357	0.2252	
AD	6.05E-07	1	6.05E-07	2.056089	0.1619	
AE	1.33E-05	1	1.33E-05	45.06827	< 0.0001	
AF	1.15E-05	1	1.15E-05	39.15065	< 0.0001	
BC	1.95E-05	1	1.95E-05	66.37683	< 0.0001	
BD	3.2E-07	1	3.2E-07	1.087518	0.3054	
BE	2.76E-06	1	2.76E-06	9.38409	0.0046	
BF	9.8E-07	1	9.8E-07	3.330524	0.0780	
CD	3.13E-06	1	3.13E-06	10.62029	0.0028	
CE	4.06E-06	1	4.06E-06	13.80213	0.0008	
CF	1.8E-07	1	1.8E-07	0.611729	0.4403	
DE	5E-09	1	5E-09	0.016992	0.8972	
DF	1.01E-07	1	1.01E-07	0.344097	0.5619	

EF	1.81E-06	1	1.81E-06	6.134281	0.0191	
Residual	8.83E-06	30	2.94E-07			not
Lack of Fit	7.91E-06	23	3.44E-07	2.631841	0.0954	significant
Pure Error	9.15E-07	7	1.31E-07			
Core Total	0.000464	51				
Std. Dev.	0.000542		R <sup>2</sup>	0.980971		
Mean	0.007369		Adj R <sup>2</sup>	0.96765		
C.V. %	7.360963		Pred R <sup>2</sup>	0.930766		
PRESS	3.21E-05		Adeq Precision	35.90169		

From ANOVA test of surface crack density, it was observed that the model with a p-value of <0.0001 is statistically significant. The p-values <0.05 indicated that the linear (A, B, C, D, E, F) and interactive (AB, AE, AF, BC, BE, CD, CE, EF) model terms had considerable influence on surface crack density. The lack of fit was found to be not significant. The p-value for lack of fit was 0.0954, representing that this model suitably fit into the data. The value of predicted R<sup>2</sup> and adjusted R<sup>2</sup> was close to 1 which indicated that the observed and predicted values are highly correlated to each other. The Predicted R<sup>2</sup> of 0.9308 is in sensible accord with the Adjusted R<sup>2</sup> of 0.9677. It was observed that SCD is highly influenced by pulse-on time (A) and peak current (D) as compared to wire feed (F), gap voltage (C) and pulse-off time (B). SCD increased significantly with an increase in the value of pulse-on time.

The Analysis of variance test of recast layer thickness is summarized in Table 3.

**Table 3.** ANOVA test for recast layer thickness (RCL<sub>t</sub>)

Source	Sum of Squares	Df	Mean Square	F Value	p-value Prob > F	
Model	430.2884	21	20.48993	80.47703	< 0.0001	significant
Pulse on Time-A	220.5128	1	220.5128	866.0948	< 0.0001	
Pulse off Time-B	12.73105	1	12.73105	50.00297	< 0.0001	
Gap Voltage-C	5.218502	1	5.218502	20.49639	< 0.0001	
Peak Current-D	114.0719	1	114.0719	448.0331	< 0.0001	
Wire Tension-E	0.47073	1	0.47073	1.848856	0.1840	
Wire Feed-F	2.104452	1	2.104452	8.265527	0.0074	
AB	0.000703	1	0.000703	0.002762	0.9584	
AC	2.392578	1	2.392578	9.397184	0.0046	
AD	12.76388	1	12.76388	50.13191	< 0.0001	
AE	16.63203	1	16.63203	65.32461	< 0.0001	
AF	0.236328	1	0.236328	0.928212	0.3430	
BC	2.673828	1	2.673828	10.50183	0.0029	
BD	0.411778	1	0.411778	1.617316	0.2132	
BE	0.155403	1	0.155403	0.610367	0.4408	
BF	0.444153	1	0.444153	1.744473	0.1966	
CD	5.436753	1	5.436753	21.3536	< 0.0001	
CE	26.7729	1	26.7729	105.1543	< 0.0001	
CF	3.706003	1	3.706003	14.55584	0.0006	
DE	0.181503	1	0.181503	0.712879	0.4052	
DF	2.838153	1	2.838153	11.14724	0.0023	
EF	0.533028	1	0.533028	2.093542	0.1583	
Residual	7.638176	30	0.254606			
Lack of Fit	3.811389	23	0.165713	0.303123	0.9860	not significant
Pure Error	3.826788	7	0.546684			
Core Total	437.9266	51				
Std. Dev.	0.504585		R <sup>2</sup>	0.982558		

Mean	25.29865	Adj R <sup>2</sup>	0.970349
C.V. %	1.994513	Pred R <sup>2</sup>	0.975775
PRESS	10.60878	Adeq Precision	33.85929

The Analysis of variance test of recast layer thickness, it was observed that model with a p-value of <0.0001 is significant. The p-values <0.05 showed the considerable model terms. In this case A, B, C, D, F, AC, AD, AE, BC, CD, CE, CF, DF were considerable model terms. The "Lack of Fit F-value" of 0.30 showed that it was not important relative to the pure error. There is a 98.60% chance that this large could occur due to noise. The "Pred R<sup>2</sup>" of 0.9758 was in reasonable concurrence with the "Adj R<sup>2</sup>" of 0.9703. "Adeq Precision" measures the signal to noise ratio. A ratio larger than 4 was enviable. The ratio of 33.859 indicated an acceptable signal.

Two mathematical regression models were developed by RSM for the responses SCD and RCL<sub>t</sub> respectively and optimization of process parameters was done by PSO for each response. PSO algorithm used the regression equation 7 and 8 to find the optimum solutions for SCD and RCL<sub>t</sub> respectively.

$$\begin{aligned} \text{SCD} = & 0.442 - 0.002 * A - 0.012 * B - 0.0064 * C - 0.0008 * D + 0.033 * E - 0.0374 * F + 0.00008 * A * B + \\ & 0.00001 * A * C + 6.875E-06 * A * D - 0.0003 * A * E + 0.0003 * A * F + 0.00006 * B * C - 3.333E-06 * B * D - \\ & 0.00009 * B * E + 0.00005 * B * F + 7.812E-6 * C * D + 0.00008 * C * E + 0.00001 * C * F - 2.50E-06 * D * E - \\ & 5.625E-06 * D * F + 0.0002 * E * F \end{aligned} \quad \dots (7)$$

$$\begin{aligned} \text{RCL}_t = & 362.028 - 0.8531 * A - 1.960B - 7.738C - 4.255D + 25.838D + 5.573F + 0.0007 * A * B + 0.0341 * A * \\ & C + 0.0315 * A * D - 0.360 * A * E - 0.042 * A * F + 0.0240B * C + 0.003B * D + 0.023B * E - 0.039271B * \\ & + 0.010C * D + 0.228C * E - 0.085C * F + 0.007D * E + 0.029D * F + 0.129E * F \end{aligned} \quad \dots (8)$$

### 3.1 Single response optimization for minimum SCD, RCL<sub>t</sub> using PSO

In this research, PSO algorithm was used to find minimum surface crack density (SCD) and recast layer thickness (RCL<sub>t</sub>). MATLAB software was used to run the PSO program. PSO algorithm requires some parameters to be fixed. The maximum number of iterations was taken as 100. The objective function taken was given by Equation 7 and 8 for SCD and RCL<sub>t</sub> respectively. The convergence graph of PSO for minimization of SCD and RCL<sub>t</sub> was shown in Figure 4 a-b. The PSO parameters include number of particles, their position in the solution space, inertia factor w, c<sub>1</sub> and c<sub>2</sub> factors. In this research work population size taken was 50 which represent potential solution to the problem. The inertia factor w varies between w<sub>min</sub> and w<sub>max</sub> and c<sub>1</sub>, c<sub>2</sub> taken was 2.05.

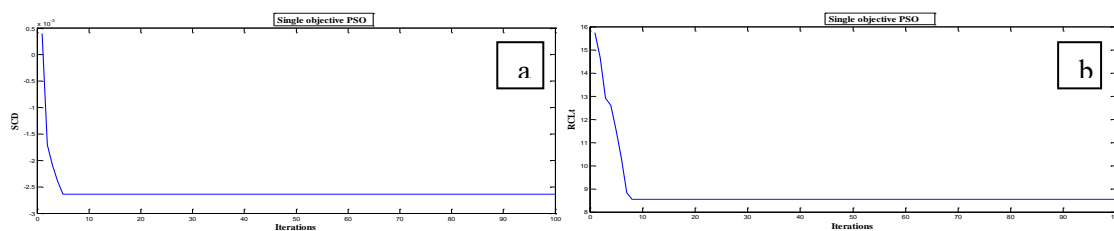


**Figure 4.** Convergence graph of PSO for minimization of (a) SCD (b) RCL<sub>t</sub>

The single-objective function (SCD) was minimized by PSO algorithm and found that T<sub>on</sub> 107 (machine unit), T<sub>off</sub> 44 (machine unit), SV 43 V, IP 113 A, WT 8 (machine unit) and WF 4 m/min as optimal process parameters for which the minimum value obtained for SCD was 0.000399 μm/μm<sup>2</sup>. The optimal conditions for RCL<sub>t</sub> i.e. T<sub>on</sub> 107 (machine unit), T<sub>off</sub> 44 (machine unit), SV 58 V, IP 110 A, WT 8 (machine unit) and WF 8 m/min and value obtained after PSO was 8.550 μm.

### 3.2 Validation of predicted results

The experiments were performed at optimum combinations for SCD and RCL<sub>t</sub>. Figure 5 showed the SEM micrograph at optimum conditions for both SCD and RCL<sub>t</sub> respectively. Table 4 showed the

comparison of results for both SCD and  $RCL_t$  respectively. At optimal combination of settings,  $0.000423 \mu\text{m}/\mu\text{m}^2$  SCD and  $8.044 \mu\text{m}$   $RCL_t$  was observed as shown in Table 4.

**Table 4:** Validation of PSO predicted model

Type of optimization	Objective	Optimization parameters						Response (Predicted)	Response (Experimental)
		$T_{on}$ (MU)	$T_{off}$ (MU)	SV (V)	IP (A)	WT (MU)	WF (m/min)		
Single objective PSO	SCD ( $\mu\text{m}/\mu\text{m}^2$ )	107	44	43	113	8	4	0.000399	0.000423
Single objective PSO	$RCL_t$ ( $\mu\text{m}$ )	107	44	58	110	8	8	8.550	8.044

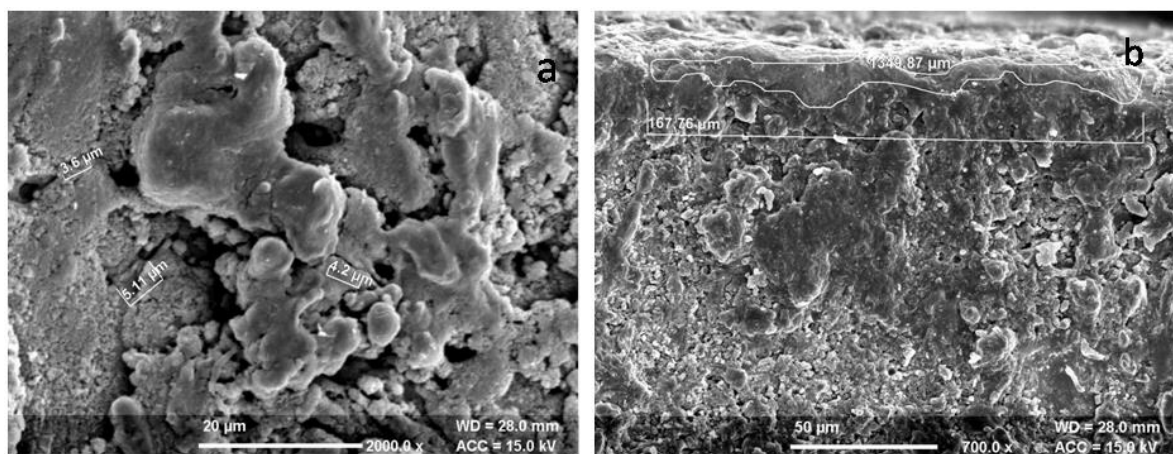


**Figure 5.** Surface crack density and recast layer thickness observed under optimized run (a) SCD (b)  $RCL_t$

It was observed from the SEM micrograph Figure 5(a-b) that at optimized condition surface topography of the machined surface is improved. This is because at low value of pulse-on time and peak current less discharge energy transferred toward the work surface and less melted material blasted from the work surface by dielectric pressure. As a result fewer craters, cracks and minimum thickness of recast layer were observed from the SEM micrograph (Figure 5a-b).

#### 4. Conclusion

WEDM machining of nickel based alloys usually disrupt the surface topography of the machined sample due to quenching process. Analysis of surface integrity of the machined surface is prone to micro-voids, micro-cracks, craters, and recast layer. It is observed from the present study that at high value of  $T_{on}$  and IP surface crack density is high while WF and WT has less significant on the SCD. Recast layer thickness is highly affected by  $T_{on}$  and IP.  $T_{off}$  and SV are found to be less significant.  $T_{on}$  110 machine unit,  $T_{off}$  43 machine unit, SV 42V, IP 115 A, WT 11 machine unit and WF 4 m/min are the optimum conditions that results in  $0.000423 \mu\text{m}/\mu\text{m}^2$  SCD and  $T_{on}$  107 machine unit,  $T_{off}$  33 machine unit, SV 56V, IP 139A, WT 8 machine unit and WF 4 m/min are the optimum conditions that results in  $8.044 \mu\text{m}$   $RCL_t$ . The developed model can be found useful in processing of Inconel 825 for industrial applications.

## References

- [1] Thellaputta GR, Pulcharu SC, Rao CSP. Machinability of Nickel Based Superalloys: A Review. 2017 *Mater Today: Proc.* 4: 3712-3721.
- [2] Kumar P, Gupta M, Kumar V. Optimization of Process Parameters for WEDM of Inconel 825 Using Grey Relational Analysis. 2018 *Dec. Sci. Lett.* 7:405-416.
- [3] Singh A, Anandita S, Gangopadhyay S. Microstructural analysis and multi response optimization during ECM of Inconel 825 using hybrid approach. 2015 *Mater. Manuf. Proc.* 30:842-851.
- [4] Ali MY, Banu A, Bakar MA. Influence of Wire Electrical Discharge Machining (WEDM) process parameters on surface roughness. 2017 *Mater. Sci. Engg.* 290 doi:10.1088/1757-899X/290/1/012019.
- [5] Shen Y, Liu Y, Dong H, Zhang K, et al. Surface integrity of Inconel 718 in high-speed electrical discharge machining milling using air dielectric. 2017 *Int. J. Adv. Manuf. Technol.* 90:691-698.
- [6] Zhang Z, Ming W, Huang H, et al. Optimization of process parameters on surface integrity in wire electrical discharge machining of tungsten tool YG15. 2015 *Int. J. Adv. Manuf. Technol.* 81:1303–1317.
- [7] Kanlayasiri K and Boonmung S. Effects of wire-EDM machining variables on surface roughness of newly developed DC 53 die steel: Design of experiments and regression model. 2007 *J. Mater. Proc. Technol.* 192-193:459-464.
- [8] Chen Z, Moverare J, Peng RL, Johansson S. Surface Integrity and Fatigue Performance of Inconel 718 in Wire Electrical Discharge Machining. 2016 *Procedia CIRP* 45:307-310.
- [9] Puri AB, Bhattacharyya B. Modeling and analysis of white layer depth in a wire-cut EDM process through response surface methodology. 2005 *Int. J. Adv. Manuf. Technol.* 25(3-4):301–307.
- [10] Rajyalakshmi G, Venkata PA. Parametric optimization using Taguchi method: effect of WEDM parameters on surface roughness machining on Inconel 825. 2012 *Elixir Int. J.* 43: 6669-6674.
- [11] Çaydas U, Ay M. WEDM cutting of Inconel 718 nickel-based superalloy: effects of cutting parameters on the cutting quality. 2016 *Mater. Technol.* 1: 117–125.
- [12] Talla G, Gangopadhyay S. Effect of impregnated powder materials on surface integrity aspects of Inconel 625 during electrical discharge machining. 2016 *Proc IMechE Part B: J Engg. Manuf.* DOI: 10.1177/0954405416666904
- [13] Goyal A. Investigation of Material removal rate and Surface roughness during Wire electrical discharge machining (WEDM) machining of Inconel 625 super alloy by cryogenic treated tool electrode. 2017 *J. King Saud Univ.Sci.* doi:http://dx.doi.org/10.1016/j.jksus.2017.06.005.
- [14] Sharma P, Chakradhar D, Narendranath S. Evaluation of WEDM performance characteristics of Inconel 706 for turbine disk application. 2018 *Mater. Design* 88:558–566.
- [15] Kennedy J, Eberhart R. Particle swarm optimization. 1995 IEEE International Conference on Neural Networks 1942–1948.